A 3D NONLINEAR DYNAMIC ANALYSIS OF A ROCK-FILL DAM BASED ON IZIIS SOFTWARE

VIOLETA J. MIRCEVSKA, VLADIMIR BICKOVSKI and MIHAIL GAREVSKI

about the authors

Violeta J. Mircevska
University "St. Cyril and Methodius",
Institute of Earthquake Engineering and Engineering Seismology,
Salvador Aljende 73,
P.O. Box101, 1000 Skopje, Macedonia
E-mail: violeta@pluto.iziis.ukim.edu.mk

Vladimir Bickovski
University "St. Cyril and Methodius",
Institute of Earthquake Engineering and Engineering Seismology,
Salvador Aljende 73,
P.O. Box101, 1000 Skopje, Macedonia
E-mail: bickovski@pluto.iziis.ukim.edu.mk

Mihail Garevski
University "St. Cyril and Methodius",
Institute of Earthquake Engineering and Engineering Seismology,
Salvador Aljende 73,
P.O. Box101, 1000 Skopje, Macedonia
E-mail: garevski@pluto.iziis.ukim.edu.mk

abstract

This paper treats the 3D nonlinear dynamic behavior of a rock-fill dam based on the Mohr-Coulomb failure criterion. The dam is situated in a steep, narrow, "V-shaped" rigid canyon. The concept of a massless rock foundation is treated, for which a certain part of the rock is included in the model. The dam-rock interface was modeled by contact elements, which allowed certain relative displacements between the two media of different stiffnesses. The generation of the 3D mathematical model was related to the topology of the terrain, and the nonlinear dynamic response was based on the "step-by-step" linear-acceleration direct-integration method, making use of the Wilson-θ method. The convergence process was in accordance with the Newton-Raphson method. First, the initial static effective stresses existing in the conditions of the established stationary filtration through the clayey core were defined. The analysis was based on an original FE program for the static and dynamic analyses of rock-fill dams, as well as a FE program for the solution of the stationary filtration process through the clayey core. The dynamic response of the 3D model of the dam was defined for the effect of harmonic excitations. Dynamic analyses in the linear and nonlinear domains were performed for the purpose of comparing the results. The time histories of the linear and nonlinear responses were defined for selected sections and nodes of the model, the tension cut-off zones, the plastic deformations, and the stress-shear strain relationships. The coefficient against the sliding of the potential sliding surfaces was also defined. It can be concluded that 3D analyses as well as a nonlinear material treatment of the soils built in the dam are imperative for a proper assessment of the stability of rock-fill dams situated in narrow canyons.

keywords

automatic generation of 3D model, rock-fill dam, nonlinear dynamic analysis, elastic perfectly plastic criterion, tension cutoff, cracking zones, plastic deformations, stability

1 INTRODUCTION

This paper treats the 3D nonlinear dynamic response of a rock-fill dam with a central clayey core based on the application of the Mohr-Coulomb linear elasto-plastic criterion [4],[5]. The associated flow rule is accepted for the clay in the core, for which the failure criterion and the yielding surface are identical. In this case the shape of the yielding surface in the High-Westergaard's space is dependent only on the model's plasticity parameters, C and φ. The non-associated flow rule is accepted for the filters and the stone detritus, for which in addition to the yield function the plastic potential function is treated. The plastic potential is a function of the third plasticity parameter, the dilatancy angle ψ, used to control the inelastic volume increase as a result of the compressive stress increase after achieving the failure state.

The Mohr-Coulomb parameters can be evaluated by conventional laboratory tests, which makes their application easier. In fact, owing to its extreme simplicity and good accuracy, the Mohr-Coulomb linear elastic–perfectly plastic criterion [3],[4],[5] combined with the principle of tension cut-off [6] is used to predict the nonlinear behavior of the soils built in the dam, during the dynamic response. However, this failure criterion has two main shortcomings [5]. First, it assumes that the intermediate principal stress has no influence on the failure, which gives an unrealistic estimation of the shear strength under general loading conditions (except for triaxial compression conditions). This can, however, be overcome by the use of the SMP criterion [9]. The second disadvantage is that the meridians of the yielding surface are straight lines, which implies that the strength parameter φ does not change with the confining pressure, just like most of the other nonlinear methods for analyses [11],[12],[13],[14]. However, these two effects have an opposite impact to the shear strength: while with an increase in the confining pressure, the parameter φ decreases, and thus the shear strength decreases, the intermediate principal stress tends to increase the shear strength.

Very little has been done to reveal the dynamic behavior of rock-fill dams in typical 3D conditions, [16],[17],[18], [19],[20],[21], from the practical point of view. The analyses based on use of the QUAD-4 or FLUSH programs and their later modifications are of the shear-beam type, i.e., they do not define the residual displacements of the dam after the dynamic effect. During the dynamic effects, the developed tensile stresses can be sustained only by the clayey core of the rock-fill dams due to the cohesive properties of the clay. The development of fine cracks and the definition of the tension cut-off zones in the clayey core during the dynamic response of the dam are important for an evaluation of the dam's stability.

The contact elements are used to model more realistically the dam-rock interface, in this way preventing an unrealistic increase in the tensile stresses at the dam-rock interface and in the parts of the dam close to the support. The role of the contact elements interposed between the rock and the dam is to permit a smoother transition of the stresses in the zone of contact, allowing some differential movements in compliance with Coulomb's friction law and in accordance with the experimentally defined values of the frictional parameters C and φ at the dam-rock interface.

In the presented analysis the effect of the dam-foundation dynamic interaction is represented by the use of the most simple, conventional massless-foundation method (Wilson, 2002). Accordingly, only the effect of the foundation's flexibility is considered, while the inertia forces within the foundation's mass are neglected.

Due to the absence of any wave propagation the earthquake motion that is applied directly at the fixed boundaries is transmitted to the base of the dam without any changes. The massless concept requires the foundation's mass to be extended at least one dam height in the upstream, downstream and downward directions. The size of the massless foundation need not be very large, so long as it provides a reasonable estimate of the flexibility of the foundation rock and sufficient elimination of the boundary conditions' effect on the deformation, the stresses and the natural frequencies of the dam.

The distribution of stresses and strains in the dam body is directly affected by the profile of the canyon where the dam is situated. If a rock-fill dam is built in a narrow, ''V'-shaped" canyon, then only the sections in the central part act in plane-strain conditions. The closer the sections are to the abutments, the greater is the influence of the boundary conditions on the distribution of stresses and strains in these sections. This results in a deviation from plane-strain state conditions, followed by a decreased intensity of the spherical stress and hence a reduced shear resistance of the soil in these parts of the dam. Therefore, the behavior and the assessment of the stability of the central section based on a plain-strain analysis cannot be representative of the stability of the whole of the dam. The application of the 3D mathematical model that should be, from an engineering point of view, an appropriate and correct approximation of the real structure becomes a necessity. It is because of this that an original methodology and computer program for automatic generation was implemented, whereby the 3D model is connected with the contour lines of the terrain.

We have elaborated our own computer program, PROC3DN, for 3D static and dynamic analyses of earth-fill dams and geotechnical structures, theoretically based on [1],[2], as well as on the application of the Mohr-Coulomb failure criterion [3],[4],[5].[6].

2 AUTOMATIC GENERATION OF THE 3D MODEL OF THE DAM

The automatic generation of 3D mathematical models requires a database on the topology of the terrain in the immediate vicinity of the dam's foundation, the projected position of the axis of the dam's crest at the base, Fig. 2, and the shape of the main central cross-section, Fig. 1.

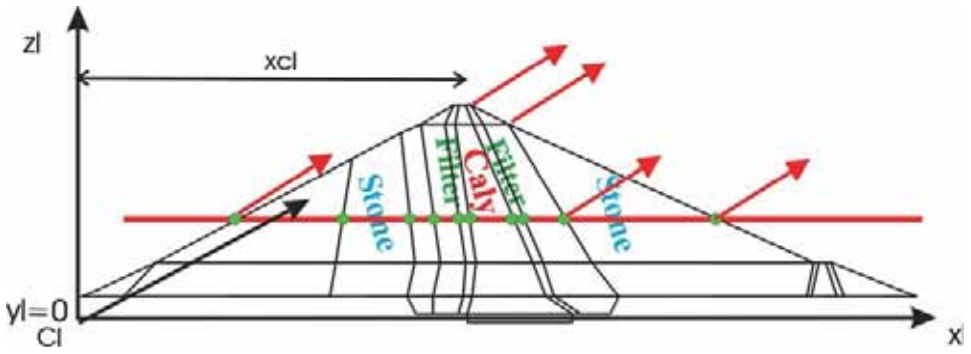

Figure 1. Main central cross-section of the dam.

The height of the dam is 127 m, which puts it in the category of high dams. The length of the dam along the crest axis is 300 m, the crest width is 10 m, and the maximum width of the base is 496 m. The clayey core has a width of 6 m at the crest and a width of 63 m at the foundation. The clayey core is founded on rock (schist). The inclinations of the upstream and downstream slopes are 1:2.2 and 1:2.0, respectively.

At each altitude the coordinates of the characteristic intersection points with the boundary lines of the plain model are defined (see Fig. 1). Drawn through these points are the straight lines parallel to the dam's crest axis. In this way the sections of the dam's body with the terrain at each altitude are obtained. A cumulative presentation of the selected horizontal cross-sections that are used for a definition of the 3D mathematical model is given in Fig. 2. The adopted 3D mathematical model, Fig. 3, has a total of 212 substructures in the dam body and 290 substructures in the rock's mass, Fig.5, 6250 external substructures' nodes, 2122 internal substructures' nodes and 2200 matrix band. The volume of the built-in clayey core is $0.338 \cdot 10^6$ m^3, while those of the filtration layers and the rock infill are $0.223 \cdot 10^6$ m^3 and $2.7 \cdot 10^6$ m^3, respectively. The dead weight of the entire structure is $G = 7.2 \cdot 10^7$ kN.

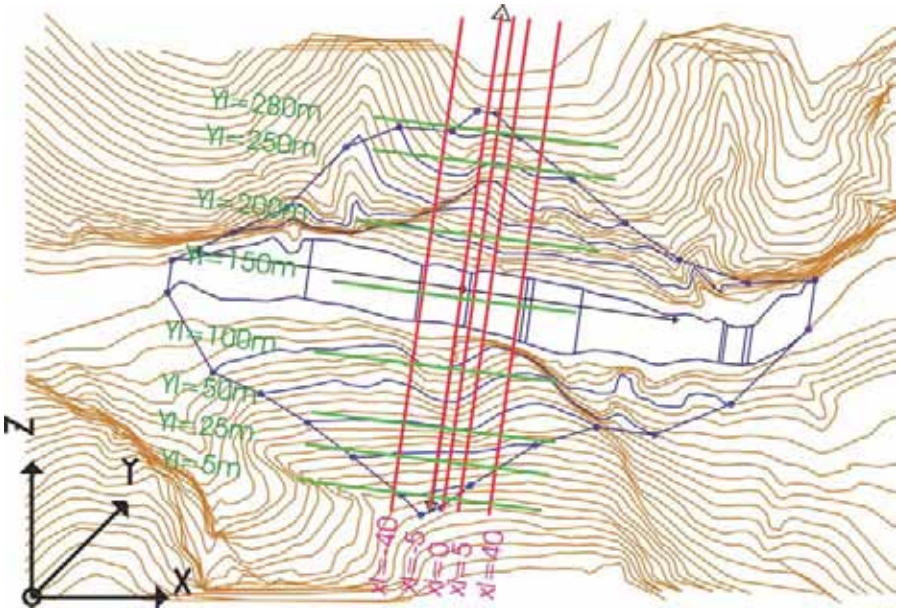

Figure 2. Plan view of the dam site with contour lines and an indication of the sections considered in the analysis.

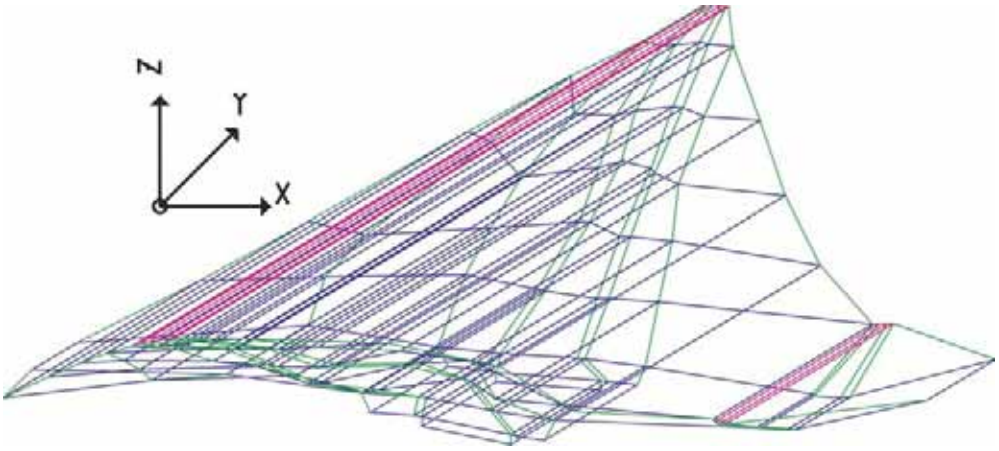

Figure 3. 3D model of the substructures adopted for the analysis.

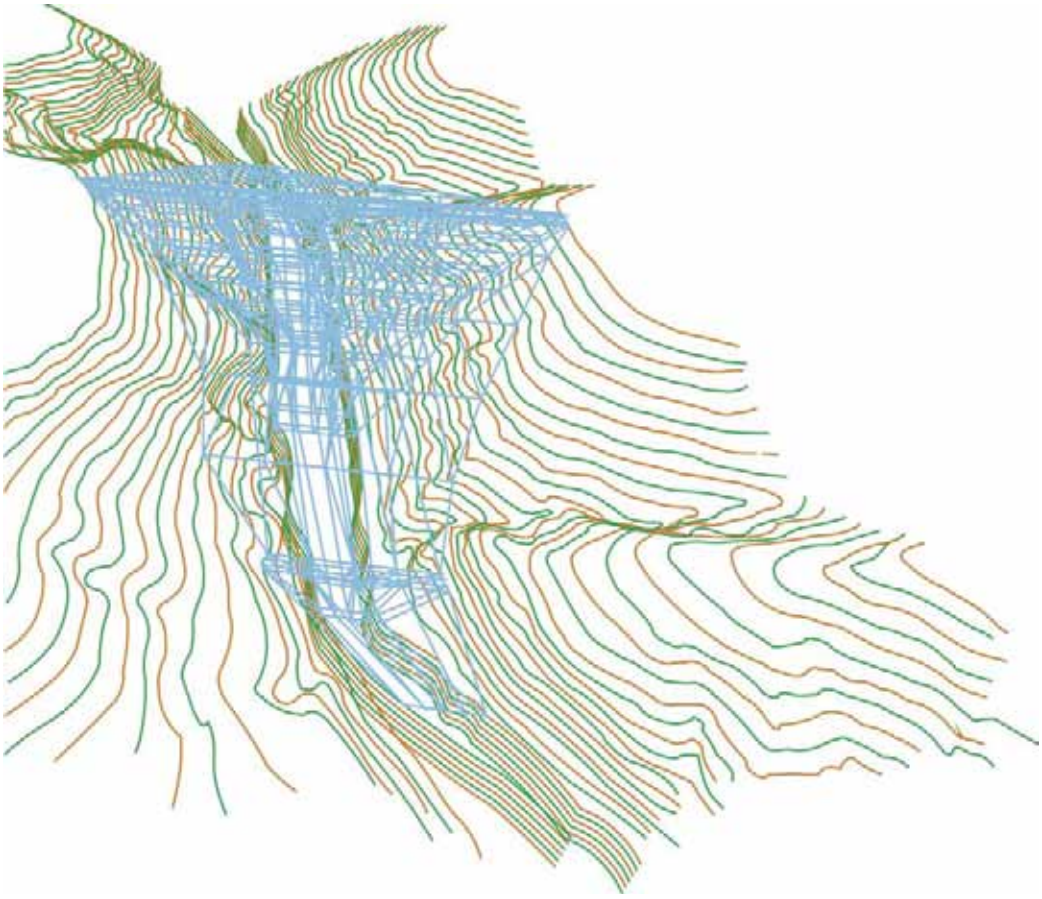

Figure 4. Perspective view of the dam and the terrain.

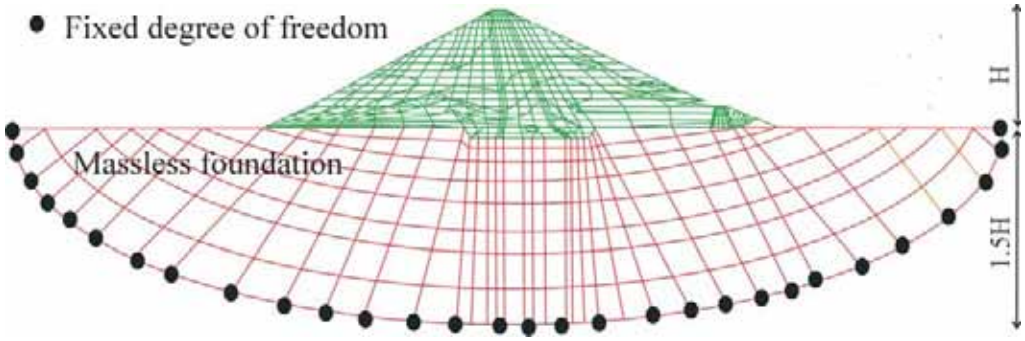

Figure 5. Rock massless model, section Yl=150 m.

3 DYNAMIC RESPONSE OF THE DAM

The dynamic response of the earth-fill dam is determined by applying the methods of modal analysis as well as by "step-by-step" direct integration, the linear acceleration method, and using linear and nonlinear analyses [7]. Within the frames of each finite element, the Newton–Raphson iterative procedure is applied in order to eliminate the vector of excessive stresses, i.e., the corresponding residual forces defined in accordance with the Mohr-Coulomb failure criterion. The main phases are as follows: solved within the frames of each i-th time step, and each iteration, is the incremental differential equation of dynamic equilibrium [8], with the following form:

$$M^{**}\Delta\ddot{U}_i + C^{**}\Delta\dot{U}_i + K^{**}\Delta U_i = \Delta P_i^{**} \qquad (1)$$

Applying the substructure technique, the differential equation of motion refers only to the external nodes of the model. Defined in this way are the incremental vectors of displacement, the velocity and the acceleration at the external nodes of the system. The matrices and vectors indicated by two stars refer to the external nodes of the substructures. The dynamic response at the end of each time step is defined by summing up the dynamic response from the beginning of the time step and the effect from the iterations performed in it.

$$U_n = U_0 + \sum_{i=1}^{n}\Delta Ui \qquad \dot{U}_n = \dot{U}_0 + \sum_{i=1}^{n}\Delta\dot{U}i$$
$$\ddot{U}_n = \ddot{U}_0 + \sum_{i=1}^{n}\Delta\ddot{U}i \qquad n = 1, iter \qquad (2)$$

where *iter* is the number of iterations within the frames of each time step, $U_0, \dot{U}_0, \ddot{U}_0$ are the initial vectors of displacement, velocity and acceleration, and $\Delta U_0, \Delta\dot{U}_0, \Delta\ddot{U}_0$ are the corresponding incremental vectors.

Using the incremental displacement vector, within each iteration we define the vector of incremental strains and the corresponding vector of incremental stresses for each finite element as follows:

$$\varepsilon = \varepsilon_0 + \sum_{i=1}^{n}\Delta\varepsilon_i \qquad \sigma = \sigma_0 + \sum_{i=1}^{n}\Delta\sigma_i \qquad n = 1, iter \qquad (3)$$

where ε_0, σ_0 are the initial vectors of the strains and stresses and $\Delta\varepsilon_0, \Delta\sigma_0$ are the corresponding incremental vectors.

At the end of each iteration the stress state is reviewed for each finite element. Only those finite elements for which the stress state is in the plasticity zone are selected, i.e., the stress point in the Haigh Westergaard's stress space lies beyond the failure surface, as defined by the Mohr-Coulomb criterion. For these finite elements we define the excessive stresses as the difference between the resulting and the ultimate stresses, which for a given spherical stress tensor and a given stress path lie on the yielding surface. For such defined excessive stresses there are the corresponding residual forces. Solving again the incremental differential equation for the dynamic equilibrium, only by considering the effect of the defined residual forces from the previous iteration, the new vectors of the incremental displacements, are the strains and the stresses obtained in the course of the next iteration. Since the residual forces are applied to a system with an unchanged stiffness matrix, excessive stresses exist during each iteration, but their intensities are decreased with each successive iteration, i.e., the iterative process converges. Successive iterations are made until the excessive stresses and the corresponding residual forces are higher than the tolerance of the iterative procedure. The tolerance used in the analysis was 0.01.

4 RESULTS AND DISCUSSION

A dynamic analysis was performed for the effect of a harmonic excitation with a frequency of ω_o= 5.2 rad/sec, a peak acceleration of A_o= 0.3 g and a duration of T = 20 sec. The harmonic excitation was applied only in the direction of the global X-axis of the system. The time step of the direct integration was Δt = 0.02 sec. The damping matrix had an explicit form, according to Rayleigh's damping concept. For the purpose of defining the Rayleigh coefficients, the first two mode shapes of the free vibrations with frequencies of ω_1 = 6.61 rad/sec and ω_2 = 8.97 rad/sec and critical modal dampings of ξ_1 = 10 % and ξ_2 = 15 % were adopted. The selected harmonic excitation with a frequency close to the first fundamental mode of free vibrations of the system had a dominant dynamic factor of participation in the system's response. For the same reasons, the dynamic factor of participation for the remaining frequencies must be lower, which is confirmed by the fact that the responses obtained with the modal analysis, in which only the first mode of the system was included, and the response obtained with the direct integration method (linear analysis), point to a good correlation.

The dynamic response obtained by means of the nonlinear analysis gave a different stress-strain state for the body of the dam. The dynamic response is presented through individual finite elements at selected cross-sections, Yl = 266 m, immediately next to the right support, and Yl = 150 m, representing the central part of the dam. Figures 6 and 7 present the time histories of the developed response for relative displacements as well as the histories of the developed plastic deformations in the three global directions and the time histories of the relative velocities and the absolute accelerations developed only in the global X direction, i.e., in the direction of the applied dynamic force.

The time histories of the relative displacements suggest that the system is out of a transient state of vibration and enters into a steady state after the first two-to-three periods of the system's response. Such a fast transition from a "transient" into a "steady-state" vibration state results from the small difference between the frequencies of the exciting force and the frequency of the first fundamental mode of free vibrations of the system. At the cross-section Yl = 150 m, representing the central part of the dam characterized by a greater flexibility, the transition from a "transient" into a "steady-state" vibration state is faster than for the cross-section Yl = 266 m, which is situated in the vicinity of the support.

The difference in the relative displacements between the linear and the nonlinear analyses (direct integration) for the cross-section Yl = 266 m, immediately next to the right support, in a finite element of the contact between the stone prism and the filtering layer, on the upstream side of the dam, is 35–40 %. The extreme current values of the plastic deformations are $U_{p,x}$ = 0.0205 m in the X direction, $U_{p,y}$ = -0.034 m in the Y direction, and $U_{p,z}$ = 0.028 m in the Z direction. The element tends to undergo plastic deformation in the X direction, i.e., in the direction of the excitation action, with a tendency for vertical displacement (settlement).

Comparing the displacement responses obtained by modal analysis and direct integration (linear analysis), the differences in all three directions, particularly in the global Y and Z directions, are evident. The reason is that the participation of only the first mode shape in the modal analysis is not sufficient to provide a more accurate response (a modal truncation problem).

The difference between the relative displacements obtained by the linear and nonlinear analyses (direct integration) for the cross-section Yl = 150 m, the central part of the dam, in a finite element close to the crest, amounts to 20 % in the X direction and 43–56 % in the Z and Y directions. The extreme current values of the plastic deformations amount to $U_{p,x}$ = -0.28 m in the X direction, $U_{p,y}$ = 0.098 m in the Y direction and $U_{p,z}$ = -0.12 m in the Z direction. The element has a tendency to be plastically deformed in the direction of excitation, with a tendency for vertical displacement (settlement).

Comparing the displacement response obtained with the modal analysis and the direct integration (linear analysis) at this cross-section, it is clear that there is very good agreement for the displacements in the global X direction. The central part of the dam, as the most flexible part of the structure, has the most intensive dynamic response, whereas the first fundamental mode of free vibrations of the system has a dominant effect on the response in the global X direction.

According to the nonlinear analysis, the dynamic amplification factor at the cross-section Yl = 266 m for the chosen finite element is DAF = 1.08, while for the finite element located at the dam's crest, it is DAF = 1.36 (not presented here). According to the nonlinear analysis, the dynamic amplification factor at the cross-section Yl = 150 m at the dam's crest is DAF = 4, while at 2/3 of the core's height, it is DAF = 2.4 (not presented here). The dynamic amplification factor of the dynamic effect obtained through nonlinear analysis is smaller than that obtained by linear analysis. The residual plastic deforma-

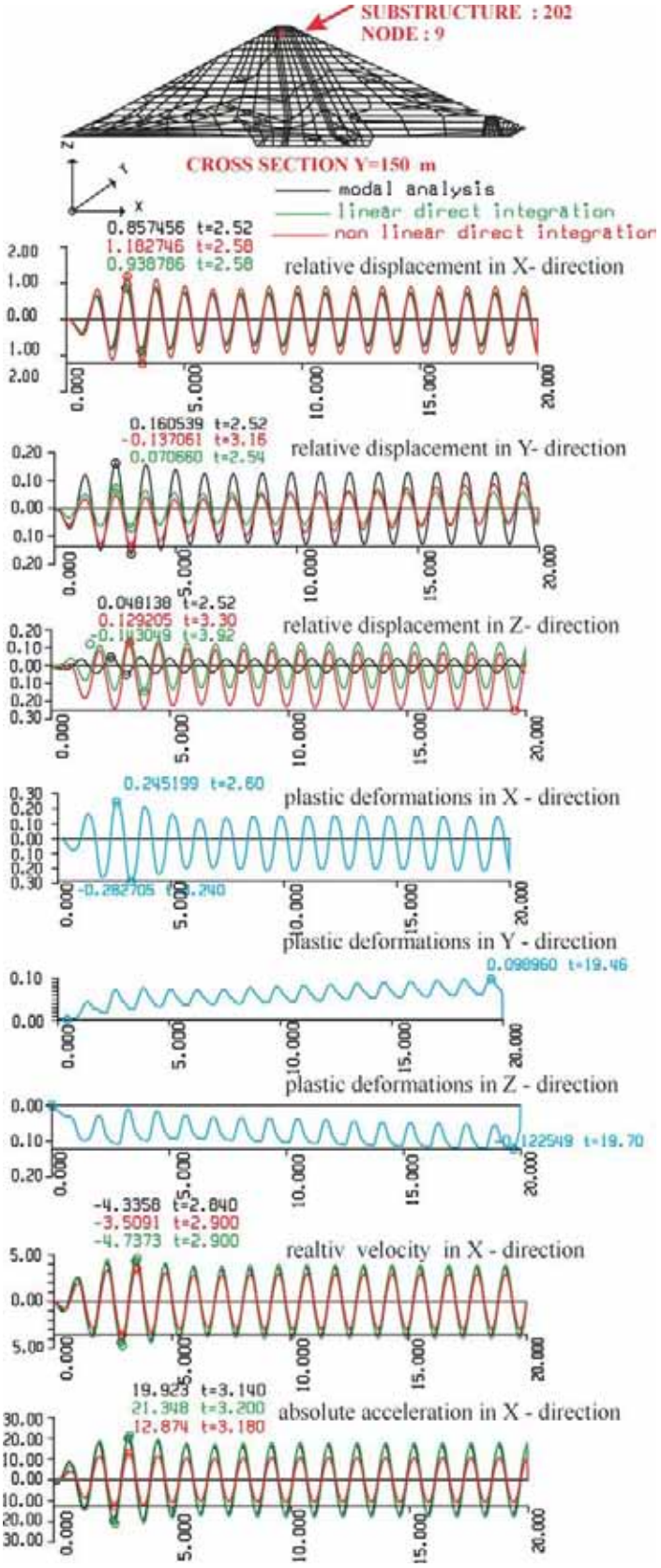

Figure 6. Time histories for a selected finite element as indicated for section Yl = 150 m.

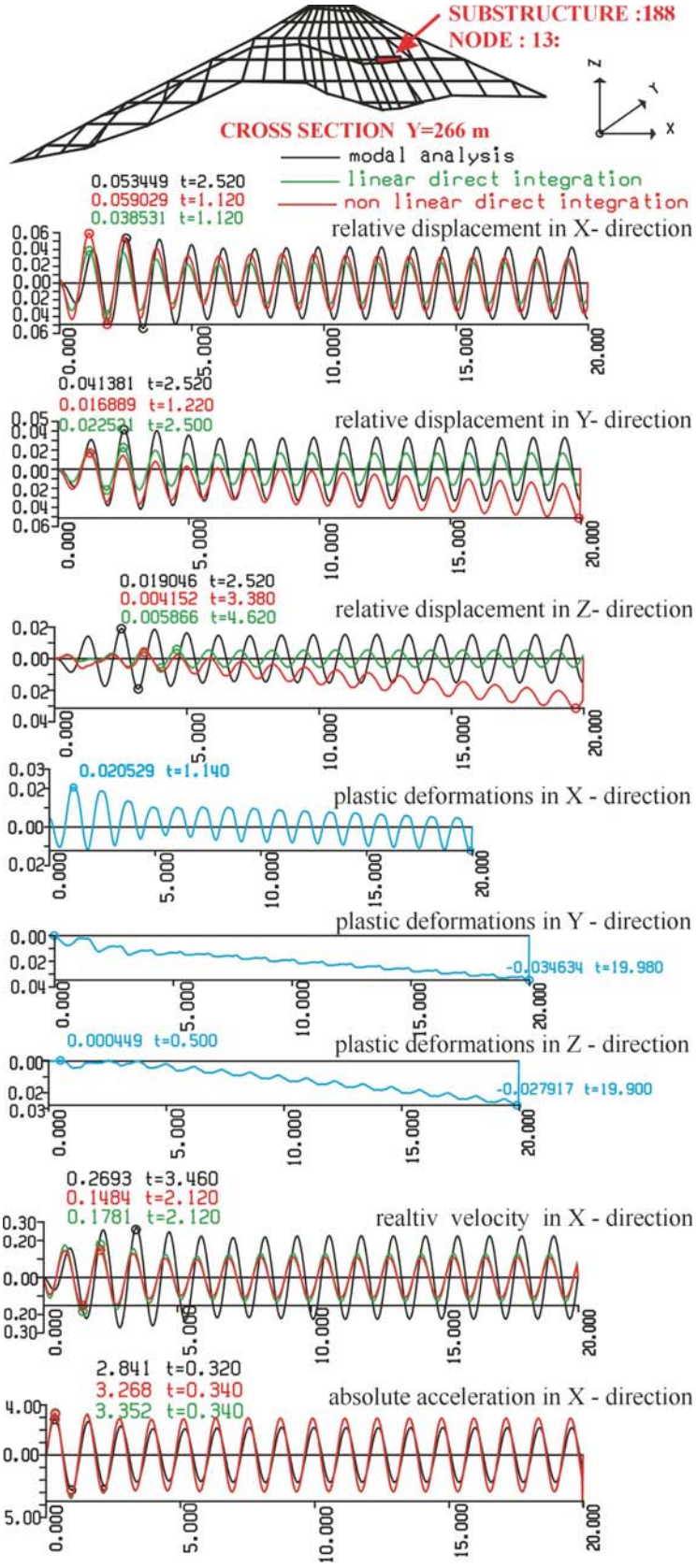

Figure 7. Time histories for a selected finite element as indicated for section Yl=226 m.

tions in the dam's body are obtained by superimposing the residual displacements in the course of the iterative processes within the frames of all the time steps. Figure 8 only shows the residual plastic deformations for the clayey core. From this we can conclude that after the effect of the harmonic excitation, the clayey core will be buckled along the dam crest, with the maximum plastic deformation in the X direction $U_{px,max}$ = -0.44 m and the maximum plastic deformation in the Z direction $U_{pz,max}$= -0.29 m. The residual plastic deformation in the Y direction, in the upper third of the core, shows a tendency to be compressed toward the central part $U_{py,max}$ = -0.16 m. Figure 9 and Fig. 10 show the plastic deformations at some chosen cross-sections of the dam. The residual plastic deformation of these cross-sections confirms the flexibility in the upper third of the core. Based on the residual plastic deformations we can conclude that there is compaction in the Z direction, i.e., settlement of the dam as a result of its nonlinear behavior during the dynamic response. Figures 11 and 12 show the time histories of the principal and component stresses for a selected finite element in the central cross-section Yl = 150 m.

A comparison has been made between the stresses obtained from the linear analysis by using the direct integration method and those obtained in the nonlinear analysis. As shown by the linear analysis, the principal stress, σ_1, is a tensile stress, which according to the Mohr-Coulomb failure criterion, cannot be sustained by the clay. The stress state, according to the nonlinear analysis, is transferred into the zone of pure compression. It is evident that there is a reduction of the component shear stresses down to the level of the allowable stresses, which are a function of the manifested spherical tensor of stresses and the stress path. The time histories of the principal and component stresses that refer to the finite elements located at the base show that the bottom of the dam is under compression, with high intensities of spherical compressive stresses and a weakly expressed nonlinearity (not presented here). Shown in Figures 13 and 14 are the component shear stress-strain relationships for chosen finite elements at the central cross-sections of the dam. The stresses and the shear strains have a lower intensity toward the supports and in the higher layers of the dam. Presented in Figs. 17 and 18 are snapshots of the nonlinear deformations for the selected sections of the dam, representing the time of manifestation of the widest zone of occurrence of cracks as a result of exceeding the allowable tensile stresses. The range of the manifested tensile strains is indicated by different colors. In the course of the dynamic response of the dam, the development of tensile strains (increases and decreases) is monitored and hence knowledge is acquired about the process of opening and closing the manifested cracks.

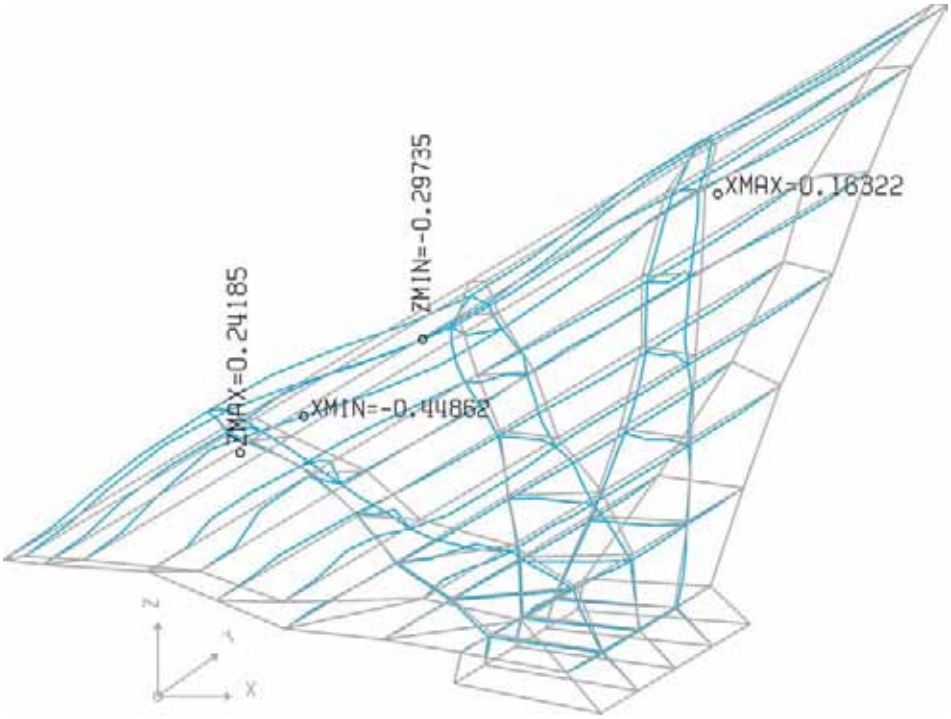

Figure 8. Plastic deformations of the clayey core.

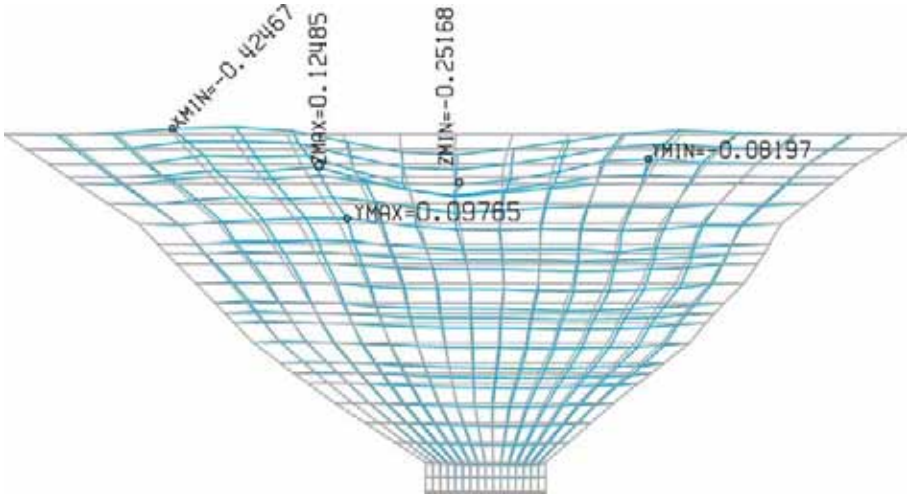

Figure 9. Plastic deformations in the longitudinal section Xl=0.

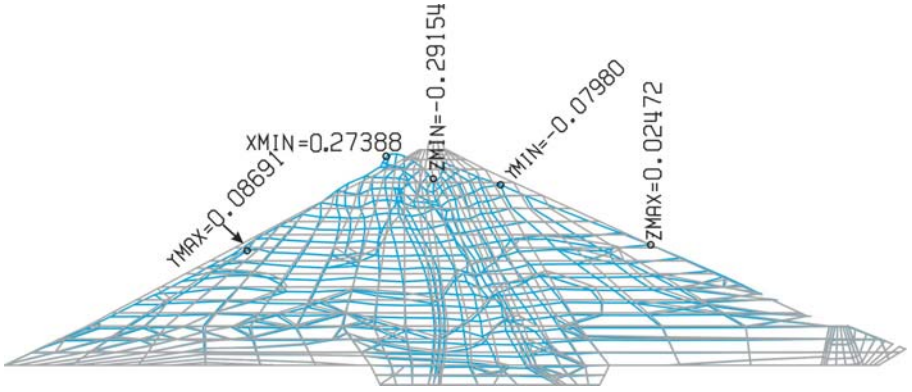

Figure 10. Plastic deformations in the central section Xl=150.

In earth-fill dams the potential sliding surfaces most frequently have the shape of a shell, so they should be defined by means of a parabola system composed of small triangles (planes), Fig. 15. The stress tensor is projected along the normal and the tangent of the elementary triangular surfaces, and with their integration the safety factor against sliding is defined. The time histories of the safety factor against sliding are defined on the basis of two performed analyses, i.e., the linear and nonlinear analyses, Fig. 16. The parameter PROB = 0.398 tells us that according to the linear analysis the potential sliding surface is unstable from 39 % of the total excitation time. According to the nonlinear analysis, the safety factor against sliding is higher than unity during the entire response time.

CONCLUSION

The profile of the canyon and the geometry of the dam structure have a predominant effect on the stress-strain state, whereby the application of a 3D mathematical model is necessary. The central part of the dam is characterized by a greater flexibility, so the transition from a transient state to a steady state of vibration is faster than with the cross-sections, which are in the vicinity of the abutments. The difference in the relative displacements between the linear analysis and the nonlinear analysis using the method of direct integration calculation for the X direction is approximately 20 % for the central part of the dam and 35–40 % for the sections toward the abutments. However, for the other two directions, this

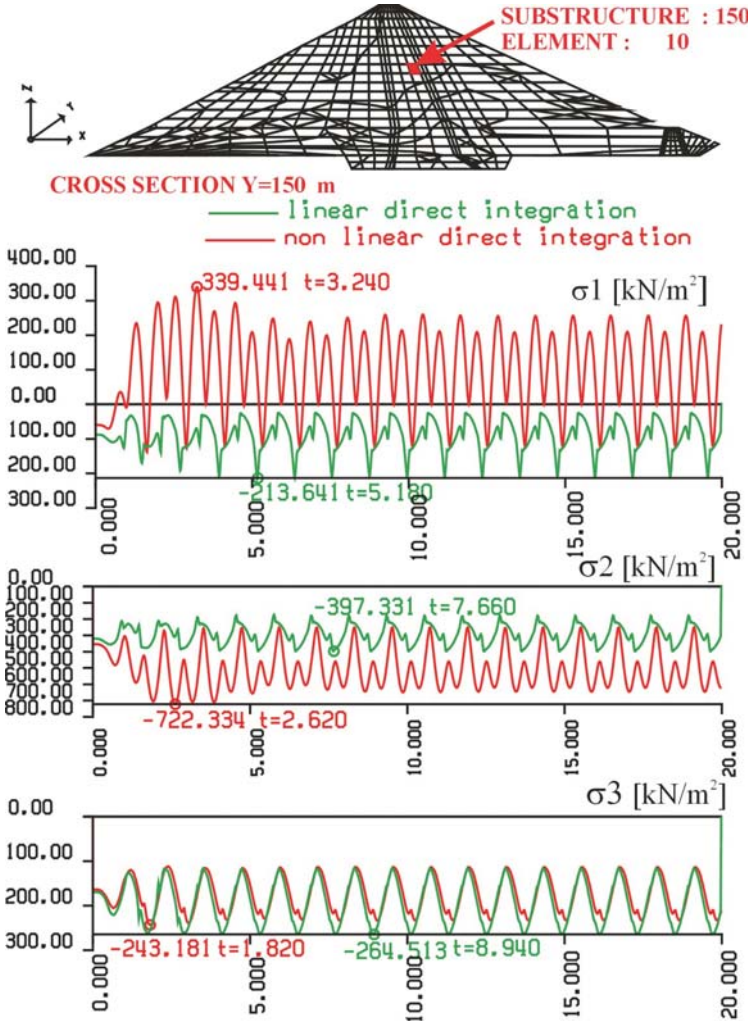

Figure 11. Time histories of the principal stresses for a selected FE for section Yl=150 m.

percentage is higher as a result of the development of larger plastic deformations, particularly in the Z direction.

The maximum value of the dynamic factor of amplification (DAF), according to the nonlinear analysis, occurs in the central part of the dam's crest, and the DAF is approximately equal to 4. However, it is smaller than the corresponding dynamic amplification factor obtained with the linear analysis. The dynamic amplification factor decreases toward the supports and with increasing depth. Under dynamic conditions the clayey core suffers plastic buckling deformations, which are particularly pronounced in the upper third of the core, because of the slender flexible core, i.e., the small dimensions in this zone. Based on the residual plastic deformations we can conclude that the settlement of the dam takes place as a result of the nonlinear dynamic response.

The component shear stresses obtained from the nonlinear analysis are lower than those obtained from the linear analysis. The reduction is down to the level of allowable octahedral shear stresses as a function of the existing spherical stress tensor. The stress state in the deepest zones of the dam is in the range of pure pressure, with a greater intensity of spherical stresses, which results in a slightly expressed nonlinearity. The shear strains are of the order of 10^{-3}, and the shear-stress/shear-strain diagrams clearly illustrate the elastic-plastic behavior of the soil media in accordance with the adopted constitutive law of nonlinearity.

According to the analysis, the time when the cracks occur can be recognized by the fact that in the time histories of all the principal stresses, the stresses are reduced to a value of $\sigma = 0$, at the same time.

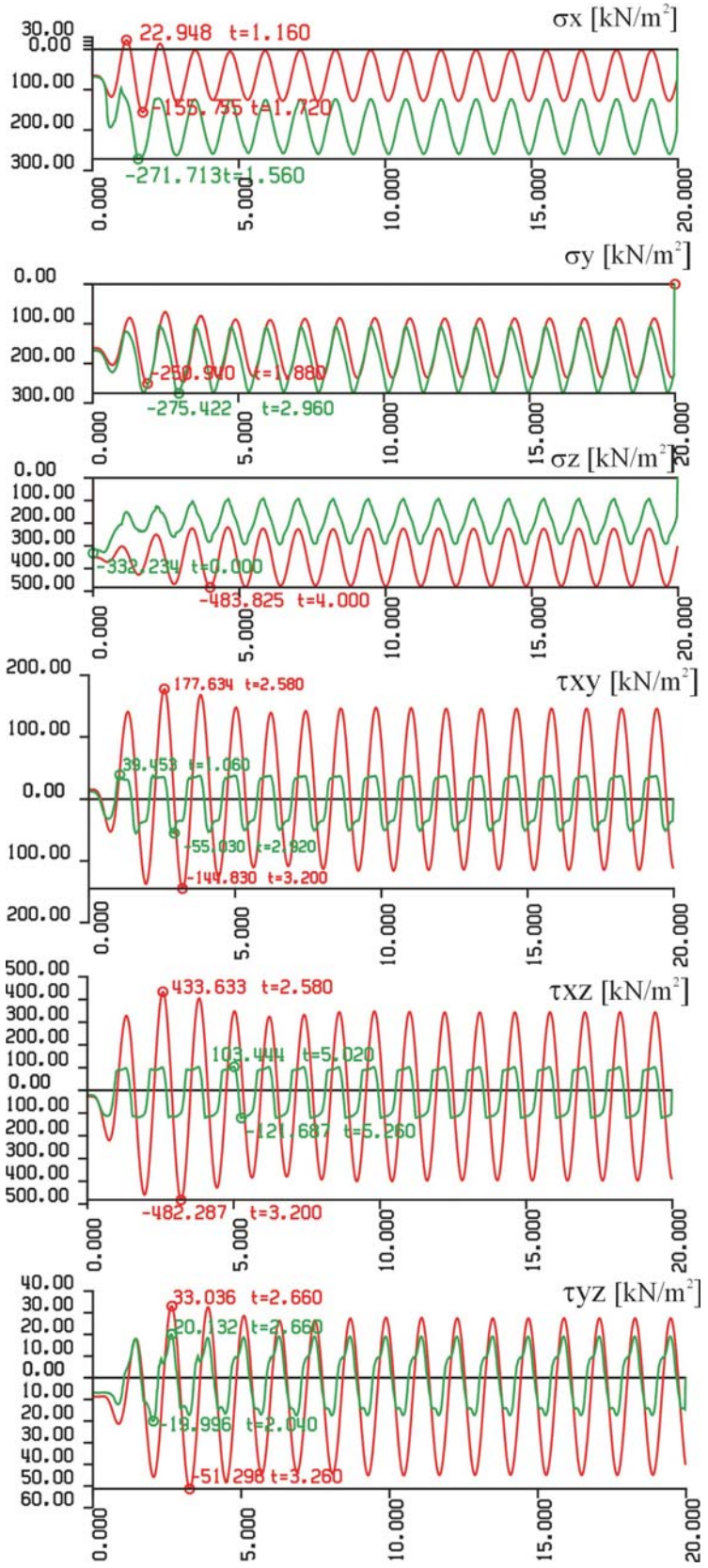

Figure 12. Time histories of the component stresses for a selected FE for section Yl=150 m.

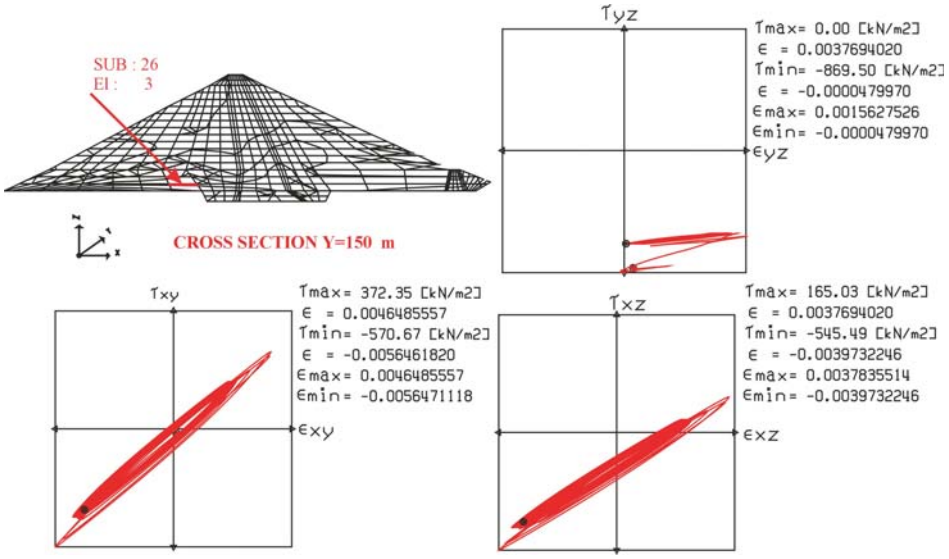

Figure 13. Shear stress-strain relationship for the chosen FE.

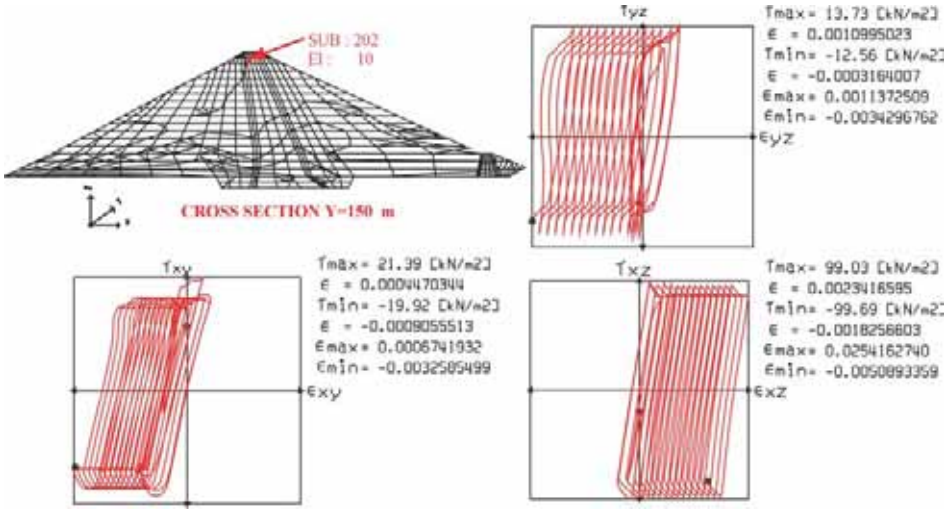

Figure 14. Shear stress-strain relationship for the chosen FE.

The mobilized strength in the analysis can achieve a value of less than or equal to unity. In the case when the element is in the zone of elastic behavior, the stress point is below the yield surface and the mobilized strength is less than unity. In the case when the element is in the zone of plastic behavior, the stress point lies on the yield surface and the mobilized strength is close to, or equal to, unity. The unit value of the mobilized strength provides information about those finite elements that exert plastic behavior. In this case any judgment about stability should be based on the resulting plastic deformations in the vicinity of such finite elements.

The safety factor against sliding defined by the linear analysis is lower than that defined by nonlinear analysis. This is due to the reduction of the active shear forces down to the level of the ultimate forces, in conditions of the existence of the ultimate plastic equilibrium.

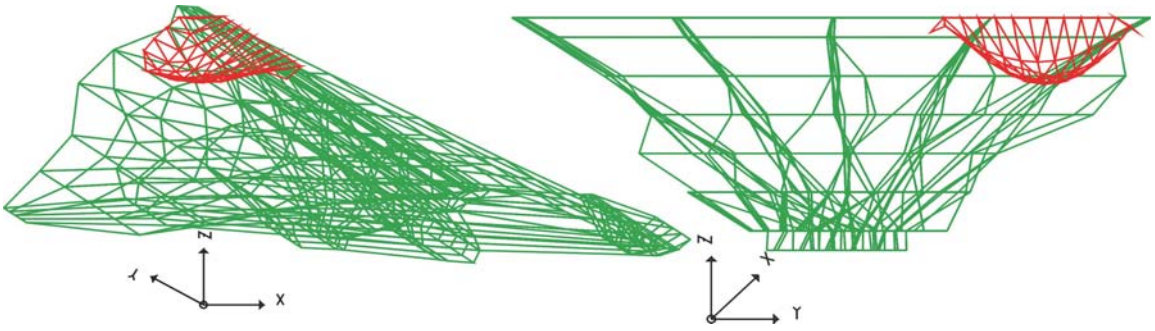

Figure 15. Position of the potential sliding surface in the dam.

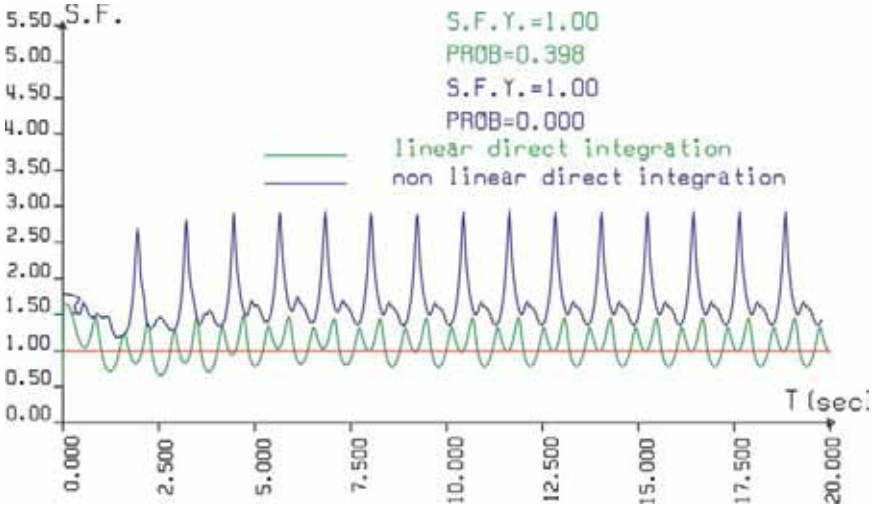

Figure 16. Time history of the safety coefficient against sliding.

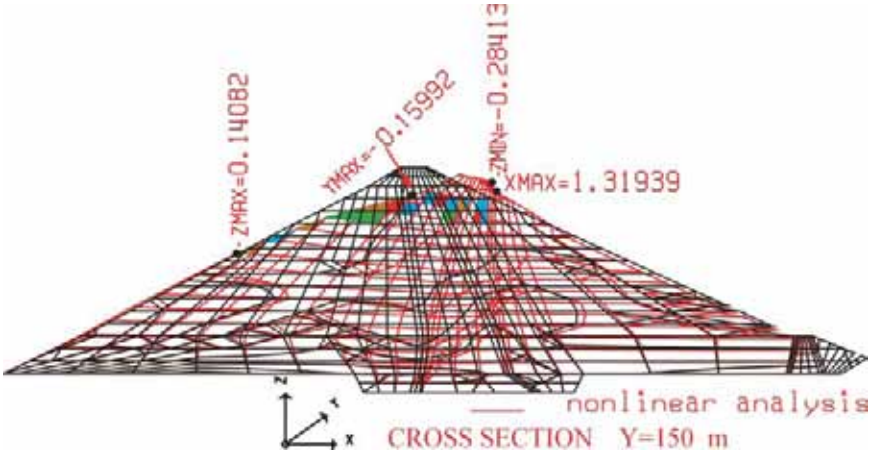

Figure 17. Snapshot T=2.58 sec. Extreme cracking zone in the section.

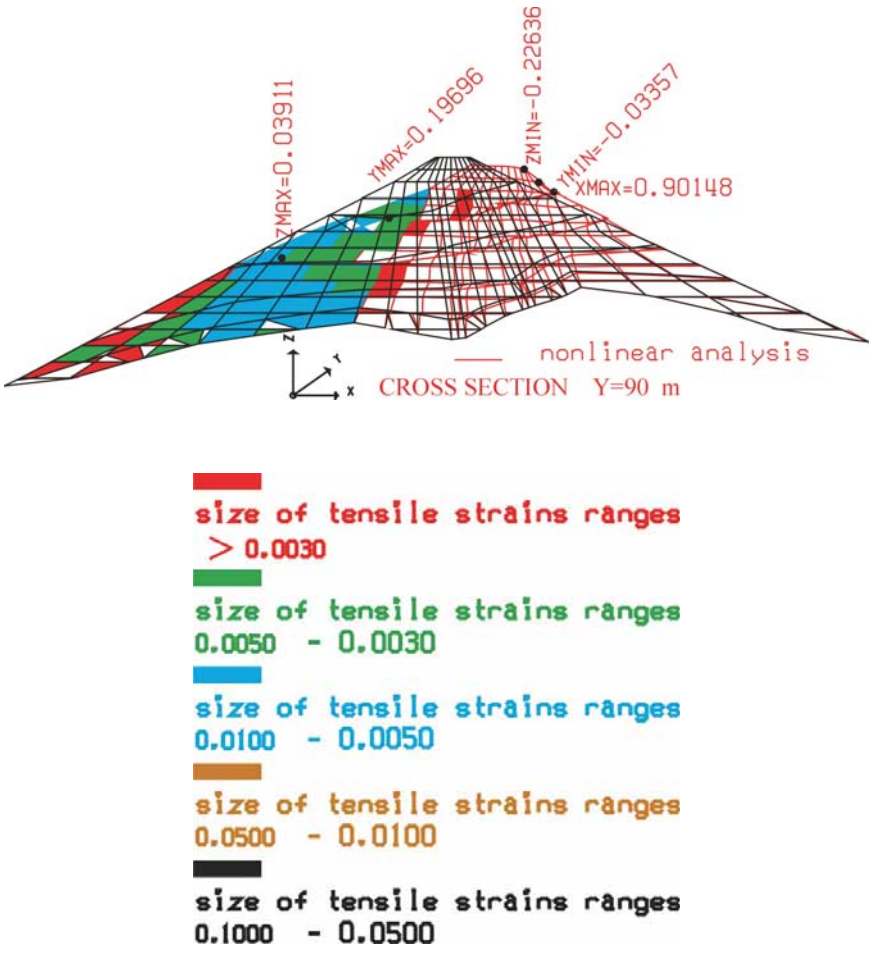

Figure 18. Snapshot T=2.66 sec. Extreme cracking zone in the section.

ACKNOWLEDGEMENT

The authors wish to express their gratitude to the Ministry of Education and Science of the Republic of Macedonia for its partial financial support of the research activities in the course of the creation of the computer program.

REFERENCES

[1] Bathe K.J. and Wilson, E.L. (1976). *Numerical Methods in Finite Element Analysis*. Prentice-Hall, Inc. Englewood cliffs, New Jersey.

[2] Bathe, K.J.(1982). *Finite Element Procedures in Engineering Analysis*. Prentice-Hall, Inc. Englewood cliffs, New Jersey.

[3] Duncan, J.M. and Chang, C.Y. (1970). Nonlinear Analysis of Stress and Strain in Soils. *Journal of Soil Mech. and Foundations Div. 96*, SM5, 1629-1653.

[4] Owen, D.R.J. and Hinton, E. (1980). *Finite Elements in Plasticity: Theory and Practice*. Pineridge Press, Swansea, U.K.

[5] Wai-Fan-Chen and Atef F. Saleeb (1982). *Constitutive Equations for Engineering Materials: Vol. 1 Elasticity and Modeling*. John Wiley&Sons.

[6] Wilson, E.L. and Clough, R.W. (1962). Dynamic Response of Step-by-step Matrix Analysis. *Proc. of the Symposium on the use of Computers in Civil Engineering*, Portugal.

[7] Clough, R.W. (1969). Analysis of Structural Vibrations and Dynamic Response. *Japan-U.S. Seminar on Matrix Methods of Structural Analysis and Design*, Japan.

[8] Paz, M. (1980). *Structural Dynamics, Theory and Computation*. Van Nostrand Reinhold Company, New York.

[9] Gazetas, G. and Dakoulas, P. (1992). Seismic Analysis and Design of Rockfill Dams: State of the Art. *Soil Dynamics and Earthquake Engineering 11*, 1, 27-61.

[10] Khoei, A.R., Azami, A.R., and.Haeri, S.M. (2004). Implementation of Plasticity Based in Dynamic Analysis of Earth and Rockfill Dams: A Comparison of Pastor-Zienkiewicz and Cap Models. *Computers and Geotechnics 31*, 5, 384-409.

[11] Idriss, I.M., Lysmer, J., Hwang, R., and Seed, H.B. (1983). Quad-4 a Computer Program for Evaluating the Seismic Response of Soil-Structure by Variable Damping Finite Element Procedures. *Report No. EERC 73-16. Univ. of California*, Berkeley.

[12] Gazetas, G. (1987). Seismic response of earth dams: some recent developments. *Soil Dynamics and Earthquake Engineering*, State of Art, 6, 1, 2–47.

[13] Prevost, J.H., Abdel - Ghaffar, A.M., and Lacy, S.J. (1985). Nonlinear dynamic analysis of earth dam: comparative study. *Journal of Geotech. Eng.* 111, 7, 882-897.

[14] Finn, W.D.L., Yogendrakumar, M.,Yoshida, N., and Yoshida, H. (1986). TARA - 3: A Program to Compute the Response of 2D Embankments and Soil-Structure Interaction Systems to Seismic : Loading. Univ. of British Columbia, Vancouver, Canada.

[15] Finn, W. D. L. (2000). State-of-the-art of geotechnical earthquake engineering practice. *Soil Dynamics and Earthquake Engineering 20*, 1-4, 1-15.

[16] Zienkiewicz, O.C., Leung, K.H., and Hintom, E. (1980). Earth Dam Analysis for Earthquakes: Numerical Solutions and Constitutive Relations for Non-linear (Damage) Analysis. *Design of Dams to Resist Earthquakes, ICE*, London, 141-156.

[17] Abdel-Ghaffar, A.M. and Elgamal, A.W.M. (1987). Elasto-plastic Seismic Response of 3-D Earth Dams: Theory and Application. Journal of Geotechnical Engineering 113, 11, 1293-1325.

[18] Dokoulas, P. (1990). Nonlinear Response of Dams Founded on Alluvial Deposit in Narrow Canyons. *JSDEE*, 9, 6, 301-312.

[19] Hayashi, M., Komada, H., and Fujiwara, Y. (1973). Three Dimensional Dynamic Response and Earthquake Resistant Design of Rock-fill Dam against Input Earthquake in Direction of Dam Axis. *Proceedings of the 5th World Conference on Earthquake Eng.*, Rome.

[20] Mejia, L.H., and Seed, H.B. (1983). Comparison of 2D and 3D Dynamic Analysis of Earth Dams. *Journal of Geotechnical Eng.* 109, 11, 1383-1398.